Proceedings of the 11th International Conference
on Computational and Mathematical Methods
in Science and Engineering, CMMSE 2011
26–30 June 2011.

Modelling Structure of Colloidal Assemblies: Methodology & Examples

Bosiljka Tadić[1], Milovan Šuvakov[2] and Gregor Trefalt[3]

[1] *Department of Theoretical Physics, Jožef Stefan Institute, Ljubljana, Slovenia*

[2] *Centre for Non-equilibrium Processes, Institute of Physics, Belgrade, Serbia*

[3] *Electronic Ceramics Department, Jožef Stefan Institute, Ljubljana, Slovenia*

emails: bosiljka.tadic@ijs.si, suvakov@gmail.com, gregor.trefalt@ijs.si

Abstract

Large-scale nanoparticle assemblies may appear in different structures, depending on the fabrication method, the parameters and the constraints controlling the self-assembly processes. Consequently, the emergent aggregates may have different physical or chemical properties, closely related with their structure at mesoscopic and global scale. We briefly discuss mathematical methodology to systematically explore structures of nanoparticle assemblies by suitable mapping onto graphs (nanoparticle networks), and present some results of the numerical modeling of the assembly processes with competing attractive–repulsive forces. In particular, we study binary colloidal aggregation, where two types of particles are binding via molecular recognition, and the aggregation of three types of charged particles with different particle sizes. We show how different structures emerge when certain parameters of the self-assembly processes are varied.

Key words: nanoparticle networks, binary colloidal aggregation, charged colloids

1 Introduction

Macroscopic assemblies of nano-particles as bulk nanostructured materials or thin films [1] may exhibit a variety of different structures and with them related collective properties [2]. These are dependent on the assembly processes [3, 4] and the variations of the relevant parameters of the assembly, which affect the interactions among the constitutive nanoparticles [5]. Therefore, the structure of the nanoparticle assembly is of key importance in bottom-up fabrication of the functional nano-material. Two segments along that line, the self-assembly process itself, and the inter-dependences between the emergent spatial arrangement of the nanoparticles with the physical (chemical) properties of the material, require theoretical modelling and numerical analysis [6].

 ISBN: 978-84-614-6167-7

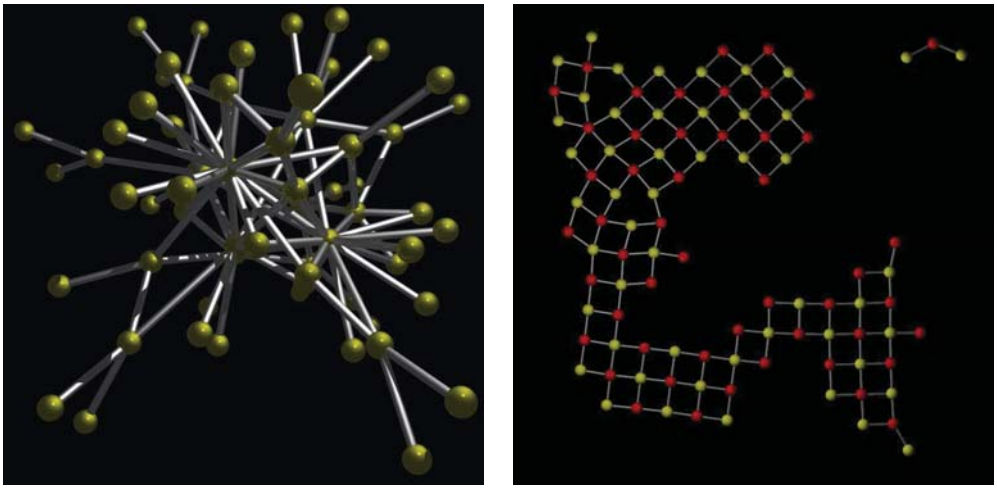

Figure 1: Examples of nanoparticle networks: (left) 3-dimensional arrangement with a scale-free graph structure [6]; (right) Regular 2-dimensional structure obtained in bio-recognition assembly (see below) with equal particle sizes and low coverage.

For the quantitative analysis of complex structures emerging in different assembly processes we have recently introduced a methodology based on mapping of the assemblies onto mathematical graphs (nanoparticle networks) and using the graph theory methods, see Refs. [7, 8, 9, 10]. Two examples of such nanoparticle networks in two- and three-dimensions are shown in Fig. 1. Nodes of these graphs are the nanoparticles, while the links indicate association of the nanoparticle pairs with a certain type of interaction. Gold nanoparticles can be ligated by bio-compatible DNA parts [3], or *functionalized* in another way to promote interaction in a given direction [11], which then affects the assembly process. In the case of charged colloidal particles, as in the case of PMN ceramics $Pb(Mg_{1/3}Nb_{2/3})O_3$ synthesis, ζ-potential can be manipulated by changing the pH of the solvent [13].

The spatial arrangements of nanoparticles of the type in Fig. 1(left) are shown to affect the processes of magnetization reversal [6, 10], which are important in the memory materials (see Fig. 2). Whereas, the planar arrangements of the metallic nanoparticles, as in Fig. 1(right), are relevant for the single-electron tunneling processes in nano-electronics [7, 9]. Both experiments and simulations in [7, 8, 9] show that the current–voltage $I--V$ characteristics strongly depend on the spatial inhomogeneity of the conducting NP films. Specifically, favorable nonlinearity is obtained in the case of stronger inhomogeneity, where the links with large topological betweenness occur. Here in section 2 we will show how several such 2-dimensional structures of the nanoparticles can arise from the self-assembly process which exploits bio-recognition binding and varied parameters. We focus on the binary colloids, where the neutral particles of two different sizes are involved. In section 3 we will also discuss the particle-size effects in the assembly processes of charged colloidal particles in 3-dimensions [13].

 ISBN: 978-84-614-6167-7

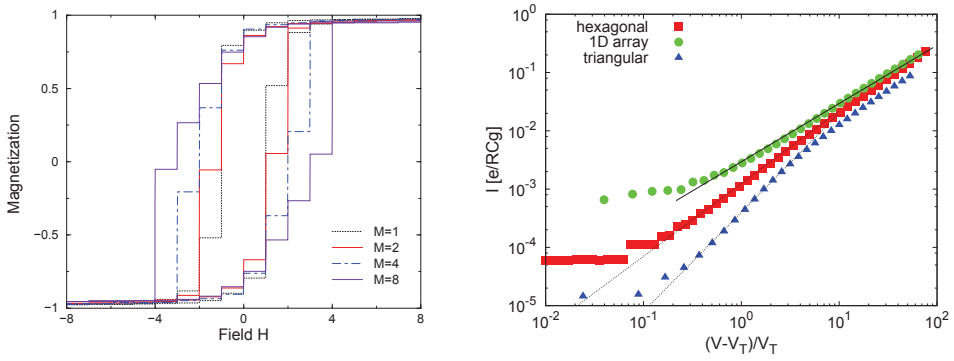

Figure 2: (left) Hysteresis loop in the magnetization-reversal on a scale-free graph, as function of the average node connectivity M [6]. (right) Current-voltage characteristics for single-electron tunneling conduction in nanoparticle films of different geometry.

2 Binary Colloidal Aggregation with Competing Forces

By attaching the biologically compatible strands of the DNA to two different nanoparticles two types of particles, A and B, can be recognized. In addition to carrying different DNA strands, the type A and type B particles in this work are assumed to be of different size, with the radius $R_A = 2.5R_B$. The bio-recognition binding can be represented by an attractive Lennard-Jones potential, with the parameters related with the binding strength (number of DNA base-pairs), the lengths of the attached DNA ligands and the particle radii [9]:

$$V_{A-B}(r) = 4\epsilon \left(\frac{\sigma^{12}}{(r - R_A - R_B)^{12}} - \frac{\sigma^{6}}{(r - R_A - R_B)^{6}} \right). \tag{1}$$

In contrast to A–B interactions, the repulsive potentials apply for the particles of the same type, $V_{X-X}(r) = 4\epsilon' \frac{\sigma'^{12}}{(r-2R_X)^{12}}$ with own parameters ϵ' and σ'^{12}.

Particle diffusion in 2-dimensional plane is simulated by solving the sets of the Langevin equations with these attractive and repulsive pair potentials and in the presence of an external random noise:

$$\nu_i \dot{\mathbf{r}}_i = -\nabla_{\mathbf{r}_i} \sum_j V_{i-j}(|\mathbf{r}_i - \mathbf{r}_j|) + \mathbf{F}_{i,T}, \tag{2}$$

where r_i is the position of ith particle and $\nu_i \equiv 6\pi\eta R_i$ represents the kinetic coefficient different for each particle type, and η is the fluid viscosity coefficient. The stochastic force $F_{i,T}$ originating from the integration over the fluid degrees of freedom, is given by the distribution with the moments $\langle F_{i,T}(t)\rangle = 0$ and $\langle F_{i,T}(t)F_{j,T}(t')\rangle = 6k_BT\nu_i\delta_{i,j}\delta_{t,t'}$.

Details of the numerical implementation can be found in [9]. Here we focus on the structures that emerge after long evolution time (lowest energy) of the assembly in different conditions. The results shown in Fig. 3 correspond to increased particle density, while the relative concentrations of the particle types are kept equal. In the low

 ISBN: 978-84-614-6167-7

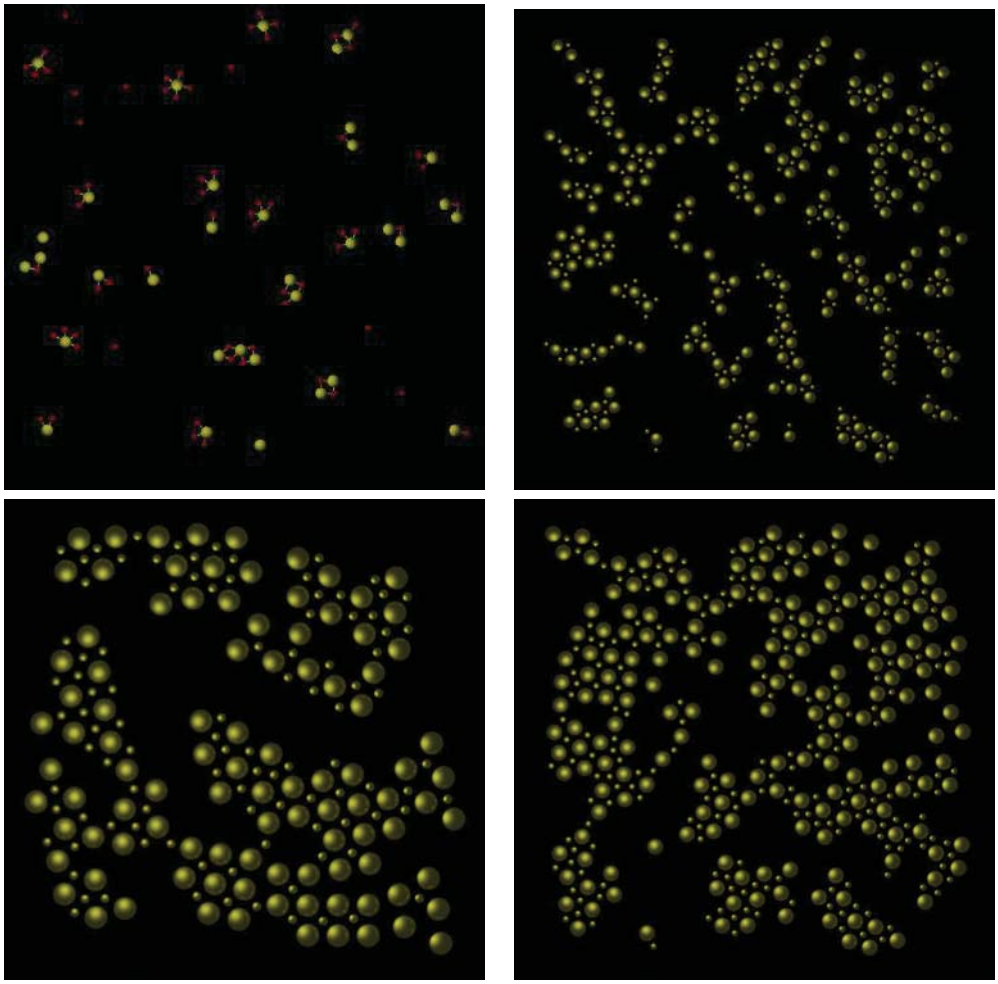

Figure 3: Emergent binary aggregates for equal concentrations and varying density.

particle density, the situation interesting for bio-sensors, a large particle appears to be isolated by six small particles. In the situations with equal concentrations, very small isolated clusters can form, as in Fig. 3 top left, where also the binding links are shown. When the density is increased, but the relative concentrations kept equal, worm-like structures appear and start joining with each other, cf. top right Fig 3. For even larger densities, areas of regular arrangements may occur with voids of different sizes between them, bottom panels in Fig 3. The large particles are cross-linked via small particles, forming a triangular pattern. Whereas, the constraint of equal concentrations prevails small particles to order at a comparable scale. Note that in the case of equal sizes of the particles, the constraint of equal concentrations leads to square lattice arrangements even at very low densities, as in the example shown in Fig. 1 right.

 ISBN: 978-84-614-6167-7

3 Size Effects in the Aggregation of Charged Colloids

As an interesting example of the aggregation of charged colloids, we consider three types of charged colloidal particles, PbO–lead oxide, MHC–magnesium hydroxy carbonate, and Nb_2O_5–niobium oxide, in the relative concentrations and the conditions relevant for the $Pb(Mg_{1/3}Nb_{2/3})O_3$ ceramic synthesis from the aqueous suspension [12, 13]. It has been found [12] that the PMN in pure perovskite phase can be synthesized when pH of the solvent is changed to pH=12.5, compared with the standard pH=11.4, where a disturbing admixture of the pyrochlore phase occurs. With the numerical model of of the system in [13] it has been shown that at pH=12.5 the polarity of the corresponding interactions change such that direct contacts between PbO and Nb_2O_5 particles, and thus the interactions leading to the pyrochlore phase, are prevented. The crucial role in this aggregation process is due to MHC particles [13]. Here we further explore the course of the aggregation at pH=12.5 with the steric effects of the MHC particles when they are prepared in different sizes. In particular, twice smaller and twice larger MCH particles compared with the other two types are considered with the Monte Carlo simulations in 3-dimensions. Snapshots of the emergent clusters are shown in Fig. 4 (MHC are shown by dark/blue color).

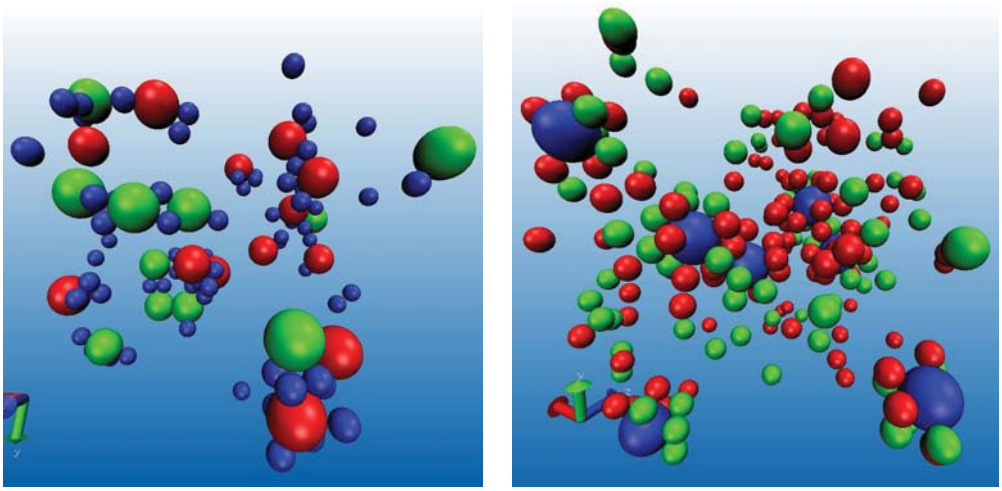

Figure 4: 3-dimensional clusters of ternary aggregates of charged colloidal particles in the model of PMN ceramics assembly at pH=12.5: Case where MHC particles are twice smaller (left) and twice larger (right) compared with PbO and Nb_2O_5 particles.

In addition to the hard-core and the van der Waals potentials, for the colloids of a given size and the type (Hamaker constant), of the key importance are the electrostatic interactions between pairs of charged particles [13]:

$$U_{ij}^{el} = \pi\varepsilon_r\varepsilon_0 \cdot \frac{a_i a_j}{a_i + a_j}\left[(\psi_i + \psi_j)^2 \ln\left(1 + e^{-\kappa h}\right) + (\psi_i - \psi_j)^2 \ln\left(1 - e^{-\kappa h}\right)\right], \qquad (3)$$

where $h = r_{ij} - (a_i + a_j)$ is the surface-to-surface distance between the particles, $\varepsilon_r\varepsilon_0$ is

 ISBN: 978-84-614-6167-7

the dielectric permittivity of the medium(the constant for water $\varepsilon_r = 78.5$ is used). ψ_i is the electrostatic surface potential of the particle i, and κ is the inverse Debye screening length $\kappa = \sqrt{\frac{2N_A e^2 I}{\varepsilon_0 \varepsilon_r kT}}$. Details of the numerical model and the implementation are given in [13]. In view of the above expressions, the steric effects due to different particle sizes is more complex, compared to the case of neutral colloids. We focus on certain features of the aggregation processes when size of the MHC particles is varied.

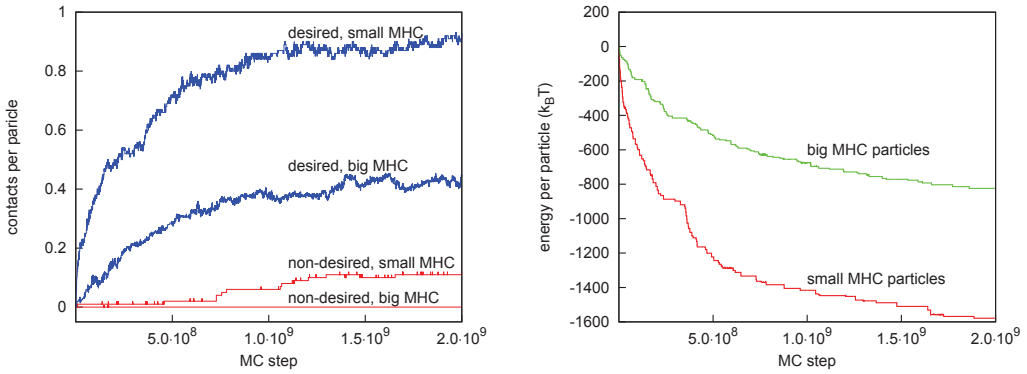

Figure 5: Energy of the assembly (right) and the fraction of "desired" and "non-desired" contacts (left) versus simulation time in the charged particle aggregation corresponding to PMN ceramic synthesis at pH=12.5, when the size of MHC particle size is varied.

In Fig. 5 we show how the number of contacts between different particle types evolves in time and the energy of the assembly. Two curves in each plot are for the situations of smaller/larger MHC particles. As mentioned above, clusters formed at pH=12.5 mostly involve MHC particles preventing direct contact $\mathrm{PbO}--\mathrm{Nb_2O_5}$. Thus "desired" contacts are $\mathrm{PbO}--MHC$ and $MHC--\mathrm{Nb_2O_5}$, while all other contact pairs might lead to unwanted chemical reactions or deteriorate the sample quality. Due to fixed concentrations of the three types of particles, the steric effect of smaller/larger MHC particles in preventing such contacts are different. For instance, for the case with smaller MHC particles a small fraction of unwanted contacts remains when the clusters are formed, while the bigger MHC are much more effective, cf. Fig. 5 left. However, from the point of view of the energy, this situation is just the opposite. In this case a large number of particles PbO and $\mathrm{Nb_2O_5}$ remain outside the clusters (cf. Fig. 4).

Acknowledgements

This work has been supported by the Research Agency Program P1-0044 and the Project PR-02485 (Slovenia) and by the National Project MNTRS 141025 (Serbia).

 ISBN: 978-84-614-6167-7

References

[1] P. Moriarty, *Nanostructured materials*, Reports on Progress in Physics **64** (2001) 297-381.

[2] M. P. Pileni, *Nanocrystal self-assemblies: Fabrication and collective properties*, J. Phys. Chem. B **105** (2001) 3358-3371.

[3] C. A. Mirkin, *Programming the assembly of two- and three-dimensional architectures with DNA and nanoscale inorganic building blocks*, Inorg. Chem. **39** (2000) 2258-2272.

[4] A. K. Boal, F. Ilhan, J. E. DeRouchey, T. Thurn-Albrecht, T. P. Russell, and V. M. Rotello, *Self-assembly of nanoparticles into structured spherical and network aggregates*, Nature **404** (2000) 746–748.

[5] C. N. Likos, *Effective interactions in soft condensed matter physics*, Physics Reports **348** (2001) 267–439.

[6] B. Tadić, *From microscopic rules to emergent cooperativity in large-scale patterns*, Ch.12 in *Systems Self-Assembly: Multidisciplinary Snapshots*, eds. N. Krasnogor *et al.*, Elsevier, Amsterdam, 2008.

[7] M. Šuvakov, B. Tadić, *Modelling Collective Charge Transport in Nanoparticle Assemblies*, J. Physics Condensed Matter: Topical Review **22** (2010) 163201-23

[8] M. O. Blunt, M. Šuvakov, F. Pulizzi, C. P. Martin, E. Pauliac-Vaujour, A. Stannard, A. W. Rushforth, B. Tadić, P. Moriarty, *Charge transport in cellular nanoparticle networks*, Nano Letters **7** (2007) 855-860.

[9] M. O. Blunt, A. Stannard, E. Pauliac-Vaujour, C. P. Martin, I. Vancea, M. Šuvakov, U. Thiele, B. Tadić, P. Moriarty, *Patterns and Pathways in Nanoparticle Self-Organization*, chapter in *The Oxford Handbook of Nanoscience and Technology*, volume I, Oxford University Press, 2010.

[10] B. Tadić, K. Malarz, K. Kulakowski, *Magnetization reversal in spin patterns with complex geometry*, Physical Review Letters **94** (2005) 137204.

[11] P. I. Archer, S. A. Santangelo, D. R. Gamelin., *Direct observation of sp-d exchange interactions in colloidal mn2+- and co2+-doped cdse quantum dots.*, Nano Letters **7** (2007) 1037-1049.

[12] G. Trefalt, B. Malič, D. Kuščer, J. Holc, M. Kosec, *Synthesis of $Pb(Mg_{1/3}Nb_{2/3})O_3$ by Self-Assembled Colloidal Aggregation*, J. Am. Ceram. Soc. (2011) DOI:10.1111/j.1551-2916.2011.04443.x.

[13] G. Trefalt, B. Tadić, M. Kosec, *Formation of Colloidal Assemblies in Suspensions for $Pb(Mg_{1/3}Nb_{2/3})O_3$ Synthesis: Monte Carlo Simulation Study*, Soft Matter (2011) DOI:10.1039/C1SM05228D.

 ISBN: 978-84-614-6167-7